焊后热处理对 Ti_3Al 电子束焊缝组织形态的影响

何景山， 张秉刚， 吴庆生， 刘 伟
（哈尔滨工业大学 现代焊接生产技术国家重点实验室，哈尔滨 150001）

何景山

摘 要：通过对 Ti_3Al—Nb 电子束焊接接头进行 650 ℃/2 h 和 1 000 ℃/2 h 的热处理，研究了两种热处理机制的电子束焊接 Ti_3Al— Nb 电子束焊缝组织形态的影响。试验结果发现 Ti_3Al— Nb 电子束焊缝中主要是 $B2$ 相的柱状晶亚结构，不同的焊后热处理机制的焊缝组织形态差异较大。1 000 ℃/2 h 热处理后焊缝为 α_2 相和 $B2$ 相相间的层片状组织（魏氏组织），650 ℃/2 h 热处理后焊缝 $B2$ 相晶界和晶内析出了少量小块状 α_2 相。两种热处理机制都将使接头区域硬度分布趋于均匀化，但 1 000 ℃热处理工艺会使接头区域硬度存在某种程度的整体软化现象。

关键词：Ti_3Al；电子束焊接；焊后热处理；显微组织
中图分类号：TG456.3 文献标识码：A 文章编号：0253— 360X(2007)05— 057— 04

0 序 言

Ti_3Al 合金高温下具有良好的高温性能，因而在航空航天等领域展现出良好的应用前景。美国已将 Ti_3Al 用于制造喷气涡轮发动机上的尾喷燃烧器、高压压气机机匣、航空发动机主排气装置的密封件及汽车的高压涡轮支撑环，并认为这种合金在未来高技术发动机上具有良好的应用前景[1,2]。此类合金其主要问题（包括室温塑性低，加工成形困难等）已经通过添加 β 相稳定元素，如 Nb，V，Mo 等进行合金化得以改善，因而其实用化过程相应提到日程上来。由于普通熔焊 Ti_3Al 合金时表现出较大的裂纹敏感性，电子束焊接 Ti_3Al 合金焊缝组织更多为单一 $B2$ 相，因而致使接头组织各区存在差异[3—8]，因此有必要通过焊后热处理使 Ti_3Al－Nb 合金焊缝区的显微组织得到改善，以期达到接头均质化处理的效果。到目前为止，对高 Nb 的 Ti_3Al 合金焊后热处理工艺对焊缝组织影响规律鲜见报到，因此文中重点研究了焊后热处理工艺对 Ti_3Al－Nb 合金电子束焊缝组织形态的影响。

1 试 验

试验采用的 Ti_3Al－Nb 合金为北京钢铁研究总院开发提供，采用真空自耗电弧炉熔炼。其化学成分如表 1 所示。

表 1 Ti_3Al－Nb 基体的化学成分（质量分数，%）

Table 1 Chemical composition of Ti_3Al-Nb

Nb	Al	Fe	Mo	Si	Cr	Cu	Mn	Ti
27.1	9.84	0.08	0.07	0.07	0.09	0.03	0.02	余量

电子束焊接试验采用从法国 TECHMETA 公司引进的 MEDARD45 型脉冲电子束焊设备，进行电子束熔透焊接，其加速电压为 60 kV，最大功率为 6 kW，试验真空度为 5.25×10^{-2} Pa。接头焊后热处理，采用从美国真空工业公司引进的 Centorr 6 —1650 —15T 真空热压炉进行，焊接接头区域利用线切割制取试样，经打磨、抛光、腐蚀制备成一系列的金相试样，所有金相试剂均采用 Kroll 试剂腐蚀。

2 试验结果与分析

2.1 电子束焊接 Ti_3Al 接头组织形态

图 1 为 Ti_3Al－Nb 合金冷轧板材的原始显微组织，$B2$ 相基体上分布着长条状或粒状 α_2 相。与基体母材相比，焊缝区域较难腐蚀。图 2 为电子束焊接 Ti_3Al－Nb 接头的微观形貌，接头区三个部分分界较为明显。

采用 XRD 对焊缝区域的相组成进行分析。图 3

收稿日期：2007— 02— 14

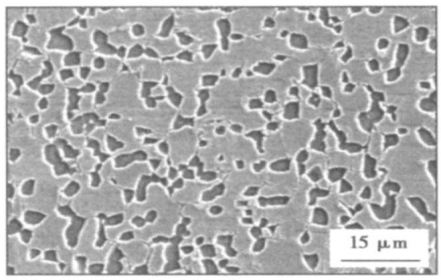

图 1 基体母材显微组织

Fig. 1 Microstructure of base metal

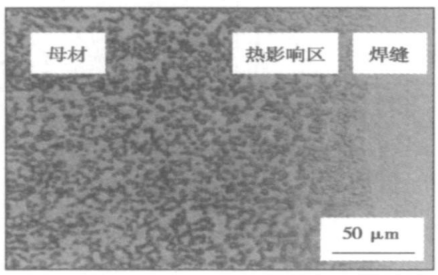

图 2 电子束焊接接头金相显微组织

Fig. 2 Optical microstructure of joint

可知，焊缝区域主要为 $B2$ 有序结构相存在，未发现 α_2，O 或 β 等其它第二相的存在，且不随焊接热输入的变化而改变。由于电子束焊接冷却速度非常快，抑制了 $\beta \rightarrow \alpha_2$ 转变，焊缝最终转变形成亚稳态的残余 β 相（$B2$）。

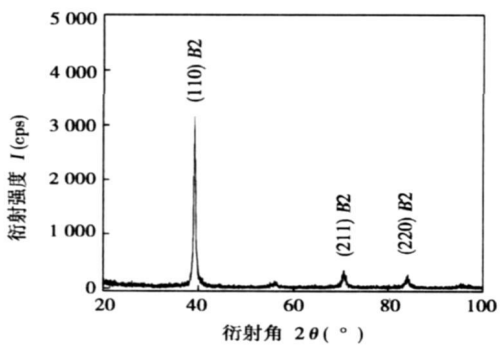

图 3 Ti_3Al－Nb 焊缝的 X 射线衍射谱

Fig. 3 X diffraction spectrum of Ti_3Al-Nb weld metal

2.2 焊后热处理参数的选择

在 Ti—Al 二元相图中选择 α_2＋β 两相区较低温度的 650 ℃和较高温度 1 000 ℃，对焊件进行 2 h 的焊后热处理，以研究焊后热处理不同机制对 Ti_3Al－Nb 合金电子束焊缝组织形态的影响。

2.3 焊后热处理对显微硬度的影响

焊后热处理接头显微硬度分布如图 4 所示。焊后热处理使试样的显微硬度更趋于均匀化。650 ℃焊后热处理的焊缝、热影响区、母材的显微硬度差别不大（336～291 HV）；而 1 000 ℃焊后热处理三区的显微硬度 232～197 HV，但接头整体存在某种程度的软化。650 ℃焊后热处理对 Ti_3Al－Nb 合金电子束焊接接头的硬度影响是由于热处理后焊缝中分解形成硬脆的 α_2 相增多，导致其显微硬度增大。而 1 000 ℃热处理后试样的显微硬度整体要比 650 ℃热处理后试样的显微硬度低，这是由于 1 000 ℃热处理后焊缝的显微组织为层片状组织，β 相晶粒长大粗化导致接头区域硬度的整体降低。

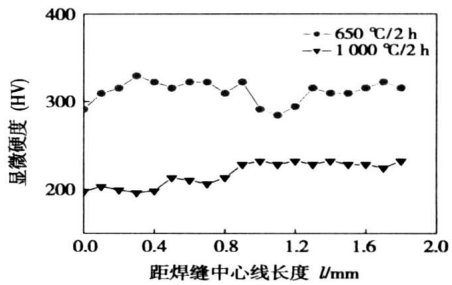

图 4 焊后热处理对接头显微硬度分布的影响

Fig. 4 Effect of post-weld heat treatment on microhardness

2.4 焊后热处理对显微组织影响

图 5 为焊后热处理接头的光学显微组织形貌。由图 5 可知，焊缝组织在原来凝固形成的 β 相柱状晶界处出现了一些半连续的第二相 α_2，β 相晶界明显，并且靠近熔合线处热影响区的晶粒比较粗大，而靠近母材处热影响区的晶粒较细小。高倍显微镜下观察发现 650，1 000 ℃和热处理后母材组织无显著变化均由 β 相基体和等轴 α_2 相组成，而焊缝组织特征有明显的不同，并且与热处理前的组织也不同。热处理前焊缝观察不到块状晶粒，而是明显的柱状晶亚结构；而热处理后就可明显观察到等轴状晶粒。

1 000 ℃热处理条件下试样的焊缝中，具有粗大等轴的原始 β 相晶粒，在原始 β 相晶界上有完整的 α_2 相网，原始 β 相晶界清晰完整，在原始 β 相晶内有长条状 α_2 相，α_2 相间夹有 β 相。β 相区内加热温度高，冷却速度慢时，容易形成平直并列的 α_2 相，并相互交错排列，而形成呈编织状的魏氏组织结构

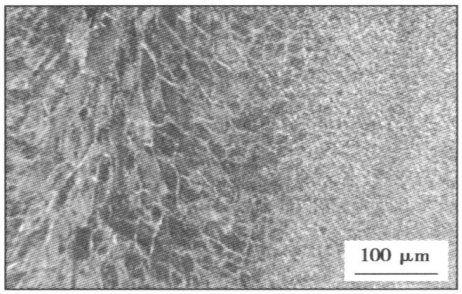

(a) 1 000 ℃/2 h

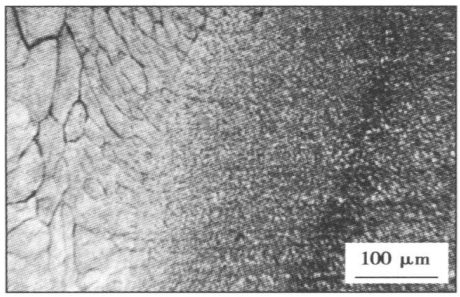

(b) 650 ℃/2 h

图 5　焊后热处理接头显微组织形貌

Fig. 5　Microstructure of joints with post-weld heat treatment

(图 6)。650 ℃焊后热处理后形成典型的等轴组织见图 7，焊缝晶粒中析出了少量的细小块状 α_2 相。

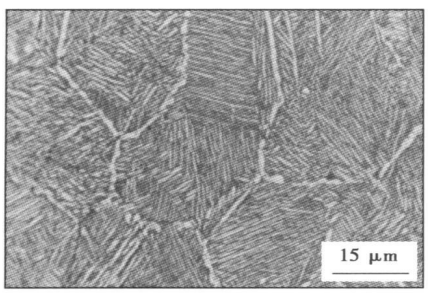

(a) 光学形貌

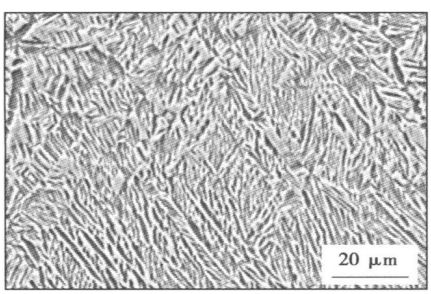

(b) SEM 形貌

图 6　1 000 ℃/2 h 热处理后焊缝微观组织形貌

Fig. 6　Microstructure of weld with 1 000 ℃/2 h heat treatment

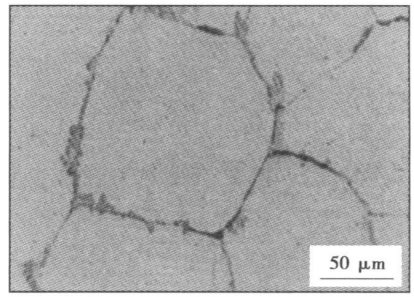

(a) 低倍形态

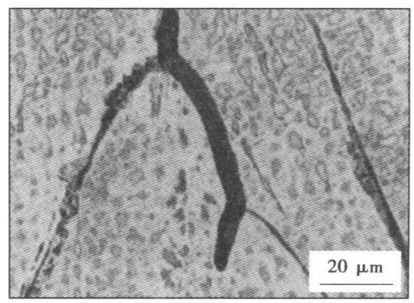

(b) 高倍形态

图 7　650 ℃/2 h 焊后热处理焊缝微观组织特征

Fig. 7　Microstructure of weld with 650 ℃/2 h heat treatment

图 8 为焊后热处理接头 X 射线衍射分析结果。

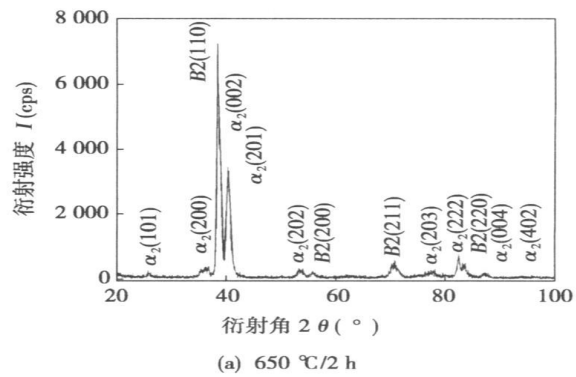

(a) 650 ℃/2 h

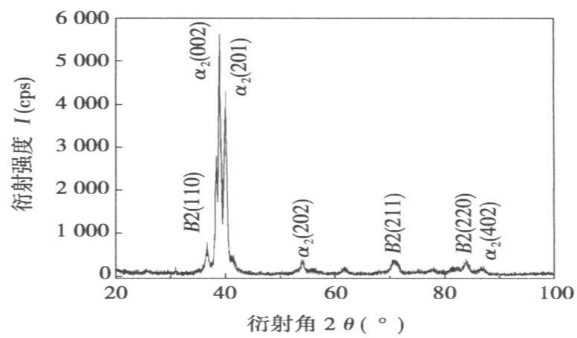

(b) 1 000 ℃/2 h

图 8　焊后热处理接头 XRD 衍射谱

Fig. 8　XRD spectrum of joints with post-weld heat treatment

焊后热处理对 Ti_3Al－Nb 合金电子束焊接接头显微组织的影响可通过焊缝中相的转变来解释。由 Ti－Al 相图可知当进行 1 000 ℃焊后热处理时已进入了 β 相区，缓慢冷却时首先在 β 相晶界处析出 α_2 相，α_2 相逐渐向晶内继续生长，生成片状 α_2 相，同时将稳定元素排挤到周围的 β 相中，使部分 β 相更加稳定而保持到室温，这样的过程不断重复进行，最终在焊缝中形成了 α_2 相和 *B*2 相相间的层片状组织。而进行的 650 ℃焊后热处理时还在 α_2＋β 相区内，α_2 相优先在晶界处析出，但由于热处理温度较低，α_2 相无法再向晶内生长，只能在晶内 *B*2 相基体上发生少量转变，生成小块状的 α_2 相组织。

从图 8 可知，Ti_3Al－Nb 合金电子束焊接热处理后焊缝是由 α_2 相和 *B*2 相组成的，相应于焊缝组织的衍射图谱，α_2 相衍射峰明显加强，而且 1 000 ℃处理后的焊缝含有较多的 α_2 相。该试验结果与上面的分析是相符的。

3 结 论

(1) Ti_3Al－Nb 电子束焊缝中主要是 *B*2 相的柱状晶亚结构，焊后热处理工艺对焊缝组织形态有重要影响。

(2) 1 000 ℃/2 h 热处理后焊缝为 α_2 相和 *B*2 相相间的层片状组织(魏氏组织)，650 ℃/2 h 热处理后焊缝为 *B*2 相晶粒的基体中析出了少量小块状 α_2 相。

(3) 两种热处理工艺都将使接头区域硬度分布趋于均匀化，但 1 000 ℃热处理工艺会使接头区域硬度存在某种程度的整体软化现象。

参考文献：

[1] 钱九红. 航空航天用新型钛合金的研究发展及应用[J]. 稀有金属，2000，24(3)：218－223.

[2] 崔约贤，甄 良，杨德庄，等. Ti－23Al－14Nb－3V 合金电子束焊接接头的显微组织及力学性能[J]. 焊接学报，1998，19(4)：130－134.

[3] Baeslack W A III, Phillips D, Scarr G K. Characterization of the weld heat-affected zone in an alpha-two titanium aluminide[J]. Materials Characterization, 1992, 28(1): 61－73.

[4] Acoff V L, Thompson R G, Griffin R D, *et al*. Effect of heat treatment on microstructure and microhardness of spot welds in Ti－26Al－11Nb[J]. Materials Science and Engineering, 1992, A152(1－2): 304－309.

[5] Martin G S, Albright C E, Jones T A. Evaluation of CO_2 laser beam welding on a Ti_3Al－Nb alloy[J]. Welding Journal, 1995, 74(2): 77－82.

[6] Baeslack W A III, Liu P S, Smith P R. Characterization of solid-state resistance welds in SiC-reinforced orthorhombic-based Ti－22Al－23Nb (at.%) titanium aluminide[J]. Materials Characterization, 1998, 41(1): 41－51.

[7] Wu A P, Zou G S, Ren J L. Microstructure and mechanical properties of Ti－24Al－17Nb(at.%) laser beam welding joints[J]. Intermetallics, 2002, 10(7): 647－652.

[8] Peter Petrov, Chavdar Georgiev, Georgy Petrov. Experimental investigation of weld pool formation in electron beam welding[J]. Vacuum, 1998, 51(3): 339－343.

作者简介：何景山，男，1963 年出生，博士，副教授。主要从事电子束焊接的科研和教学工作。发表论文 20 余篇。

Email：jingshanhlj@sohu.com

drill pipe using two-step heating process WANG Xuegang, YAN Qian, LI Xingeng (Laboratory of Special Welding and New Materials, Shandong Electric Power College, Jinan 250002, China). p53—56

Abstract: The geological drill pipe (45MnMoB steel) was joined by transient liquid phase bonding with a novel two-step heating process. The mechanical properties and microstructures of the joint were investigated, and compared with those of the joint produced by the conventional heating process. The results showed that both the heating processes produced a homogenous joint with microstructure and composition equivalent to the base metal. Compared with the conventional one-step heating process, the two-step heating process (1 250 ℃, 1 min and 1 230 ℃, 2 min) remove the dissimilar interfaces, and increased the bonded ratio, and get the joint with tensile strength of 890 MPa and bending degree of 180°, which exceeded the technical criterions of geological drill pipe. As this technology can be applied in drill pipe production without postweld machining process, and the production costs will be reduced.

Key words: geological drill pipe; 45MnMoB steel; transient liquid phase bonding; two-step heating; mechanical properties

Effect of postweld heat treatment on microstructure of electron beam welded joints of Ti_3Al HE Jingshan, ZHANG Binggang, WU Qingsheng, LIU Wei (State Key Laboratory of Advanced Welding Production Technology, Harbin Institute of Technology, Harbin 150001, China). p57—60

Abstract: The postweld heat treatment of the electron beam welded joints of Ti_3Al—Nb was carried out at 650 ℃ and 1 000 ℃ for 2 hours, respectively. Its effect on the microstructure of electron beam welded joints of Ti_3Al was investigated. Experimental results show that the microstructure of the weld under welding conditions is predominantly metastable, the columnar crystal metastructure of $B2$ phase. The microstructure of the weld is significantly influenced by the method of the heat treatment. The microstructure of the weld for postweld heat treatment at 1 000 ℃ for 2 hours is the laminar structure (Widmanstaten structure) consisted of interphase α_2 and $B2$. After postweld heat treatment at 650 ℃ for 2 hours, the small α_2 phase is precipitated in grain boundary and intragranular of $B2$ phase in the weld. After postweld heat treatment, whether 650 ℃/2 h or 1 000 ℃/2 h, the microhardness distribution of the joints are both more uniform than that of the weld without heat treatment. However, The whole joint is softened after the postweld heat treatment at 1 000 ℃ for 2 hours and the microhardness of the whole joint is not higher than that of postweld heat treatment at 650 ℃ for 2 hours.

Key words: Ti_3Al; electron beam welding; postweld heat treatment; microstructure

Thermodynamic analysis on intermediate transformation mechanism of acicular ferrite in welds XU Xiaofeng, LEI Yi (College of Mechanical and Electronic Engineering, China University of Petroleum, Dongying 257061, Shandong, China). p61—64

Abstract: Based on the fact that carbon-depleted regions come into being during the incubation period, thermodynamic models of diffusion and shear for weld acicular ferrite (AF) transformation in carbon-depleted regions of austenite were established respectively by using KRC (Kaufman, Radcliffe, Cohen) activity model and super-element algorithm, and used in the numerical simulation of a certain microalloy steel. The results show that with the variation of carbon content in the carbon-depleted region, the transformation mechanism of AF is different. The driving force in diffusion model is greater than that of shear model when the carbon content is much higher, while the driving force in shear model is a little greater than that of diffusion model when the carbon content is much lower. If there is no carbon in the carbon-depleted region, the driving forces of both models will be equal. The driving forces of the two models show the similar tendency, and increase with the decreasing of carbon content in carbon-depleted regions and AF transformation temperature.

Key words: acicular ferrite; carbon-depleted region; diffusion; shear; thermodynamics

Lap seam welding of magnesium alloy with variable polarity plasma arc JIANG Jianbo, LIU Liming, ZHU Meili, SHEN Yong (State Key Laboratory of Materials Modification, Dalian University of Technology, Dalian 116024, Liaoning, China). p65—68

Abstract: The keyhole variable polarity plasma welding was used to weld AZ31B Mg alloy, and favorable joint was obtained. The microstructure, mechanical properties and hardness were investigated by the optical microscope, tensile testing machine and hardness instrument. The results show that one side welding with back formation can be obtained through this technique when there is no groove and no enclosed protection; the heat-affected zone is narrow, and the average tensile shear is 7.3 kN; the grains of fusion zone are fine, and the hardness of welded joint is higher than that of the base metal. In summary, the variable polarity plasma arc welding process is a perfect method to weld Mg alloy, which can improve the microstructure of the joint and increase the welding quality.

Key words: keyhole variable polarity plasma welding; lap seam welding; magnesium alloy; microstructure

Ultrasonic evaluation of interface quality of TiAl and 40Cr diffusion welding LUAN Yilin, GANG Tie (State Key Laboratory of Advanced Welding Production Technology, Harbin Institute of Technology, Harbin 150001, China). p69—72

Abstract: The quality of TiAl and 40Cr diffusion welding interface was inspected by ultrasonic C-scan method and the relationships between mean and standard deviation of amplitude of interface echo and shear strength were studied. The effects of weld temperatures and surface roughnesses of specimens on above-mentioned relationships were investigated and the relationship between the amplitude and length of air gap was discussed. It is found that at a given surface roughness, bonding strength increases with the decreasing of mean and standard deviation of amplitude. The relationships between mean and standard deviation of amplitude of interface echo and shear strength are influenced by surface roughness. When the length of air gap is shorter than 400 μm, the amplitude of interface echo is approximately in proportion to the length of air gap.

Key words: ultrasonic test; C-scan; diffusion welding; dis-